Совещание по использованию рассеяния нейтронов и синхротронного излучения в конденсированных средах

27-31 октября 2014, Санкт-Петербург, Старый Петергоф

Structure and sizes of gold clusters into cucurbit [n] uril (n = 6, 7) cavities

Структура и размеры кластеров золота внутри полостей кукурбит[6,7]урила

S.B. Erenburg[1], S.V. Trubina[1], E.A. Kovalenko[1], O.A. Gerasko[1], V.I. Zaikovskii[2], V.F. Pindyurin[3], S.G. Nikitenko[4], K.O. Kvashnina[4]

[1]Nikolaev Institute of Inorganic Chemistry, SB RAS, Novosibirsk, Russia

[2]Boreskov Institute of Catalysis SB RAS, Novosibirsk, Russia

[3]Budker Institute of Nuclear Physics SB RAS, Novosibirsk, Russia

[4]ESRF, BP 220, 38043 Grenoble CEDEX 9, France

Publications

1. S. B. Erenburg, A. V. Golovin, S. P. Noskova et al. X-ray absorption K-spectra of high dispersity nickel. Reactl. Kin. Catal. Lett. 1, 507 (1974).

2. S.B. Erenburg, B.L. Moroz, N.V. Bausk, V.I. Bukhtiyarov and S. Nikitenko. XAS study on microstructure of Au nanoparticles deposited onto alumina. Nuclear Instruments and Methods in Physics Research Section A: Accelerators, Spectrometers, Detectors and Associated Equipment, 575 (2007) 105-108.

3. S.B. Erenburg, N.V. Bausk, V.V. Bakovets, I.P. Dolgovesova, V.A. Nadolinny and S. Nikitenko. Copper localization in cucurbit[*8*]uril. Nuclear Instruments and Methods in Physics Research Section A: Accelerators, Spectrometers, Detectors and Associated Equipent, 575 (2007) 88-90.

4. S. Erenburg, S. Trubina, N. Bausk, B. Moroz, A. Kalinkin, V. Bukhtiyarov, S. Nikitenko. Structure of catalytically active gold nanoparticles by XAFS spectroscopy. Journal of Physics: Conference Series, 190, (2009) 012121, doi:10.1088/1742-6596/190/1/012121.

5. S. Trubina, S. Erenburg, N.V. Bausk, V. Nadolinny, V. Bakovets, I. Dolgovesova, T. Mitkina. EXAFS and EPR spectroscopy investigation Cu(II) complexes encapsulated in cucurbit[*8*]uril. Journal of Physics: Conference Series, 190, (2009) 012128, doi:10.1088/1742-6596/190/1/012128.\

6. S. B. Erenburg, S. V. Trubina, E. A. Kovalenko, O. A. Geras’ko, V. I. Zaikovskii, K. Kvashnina, and S. G. Nikitenko. Features of the Microstructure of Gold Nanoparticles inside Cavities of Cucurbit[7]uril According to XAFS Spectra. JETP Letters, 2013, Vol. 97, No. 5, pp. 285–289.

Introduction

The physical and chemical properties of nanoparticles are known to be significantly different from the properties of the corresponding bulk materials. In particular, Au nanoparticles demonstrate high catalytic activity in reaction of low-temperature CO oxidation. This effect may be attributed to the difference in structures of "infinite" bulk materials and nanoparticles.

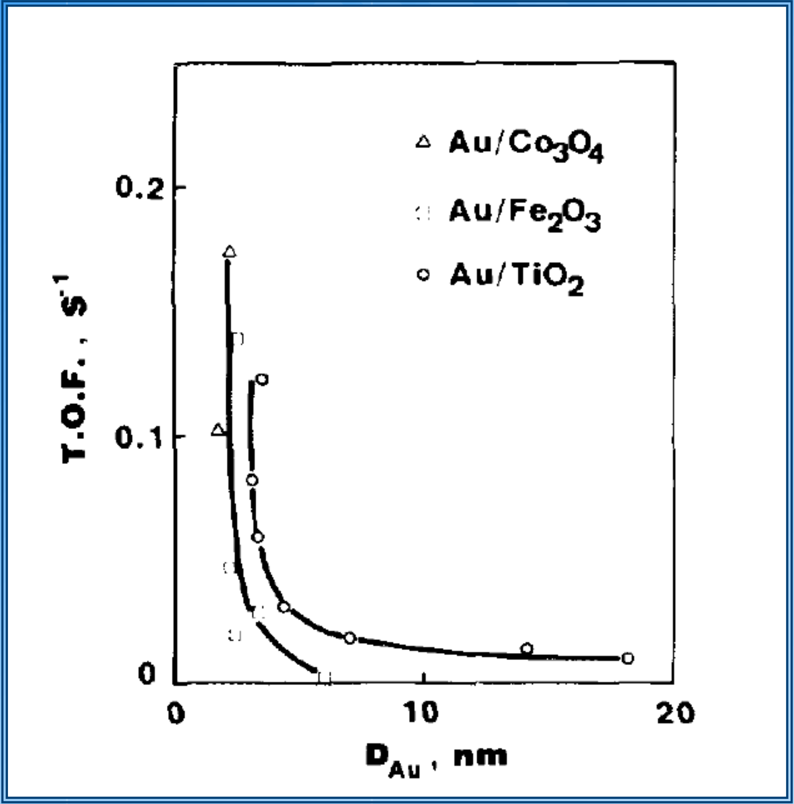

Fig. 1. *Catalytic activity in CO oxidation at 0 C based on surface gold atoms as a function of the mean gold particle diameters.*

M. Haruta et al. Low-Temperature Oxidation of CO over Gold Supported on $Ti0_2$, a-Fe_20_3, and Co_30_4. J. Catal., 144 (1993) 175.

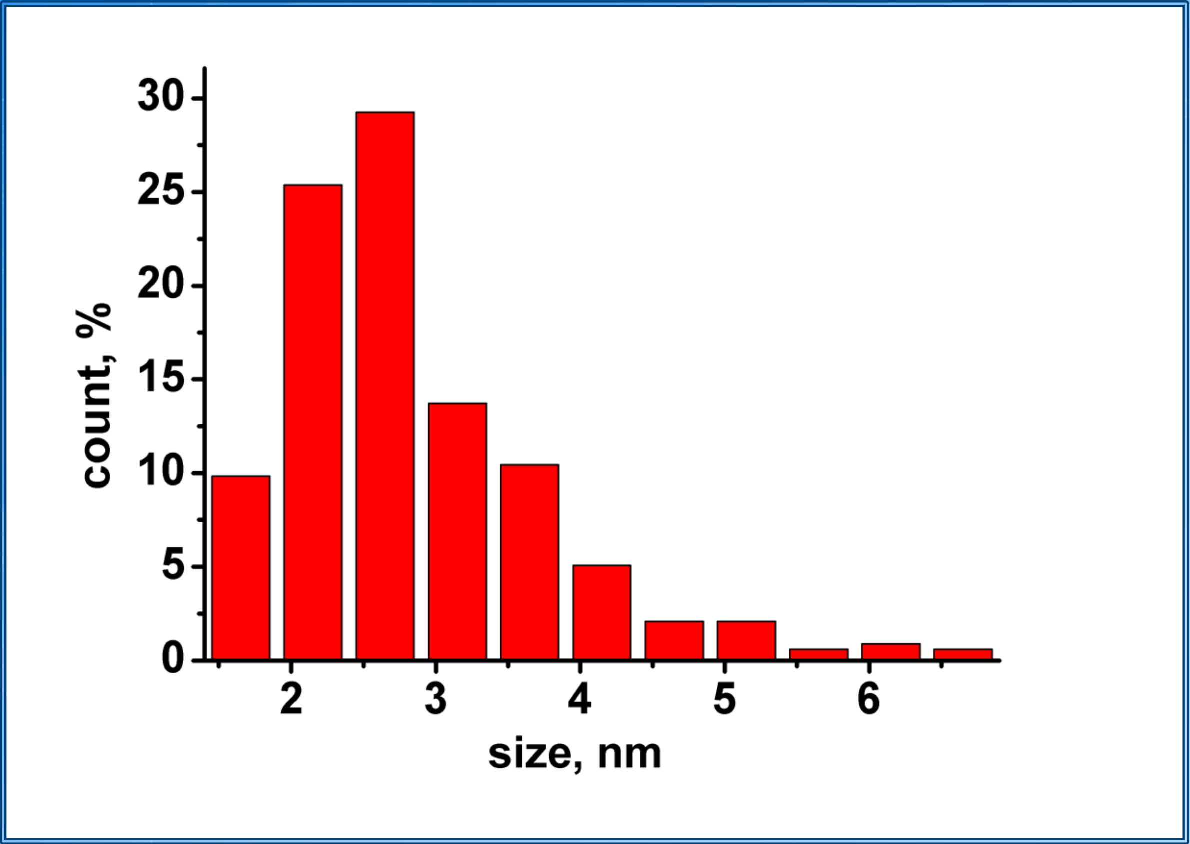

Fig. 2. *Bar chart of Au- nanoparticles size distribution calculated from TEM photo for samples Au on* Al_2O_3*, synthesized by deposition precipitation (DP) method. This sample are the more dispersed (*D_{aver}*~ 2.8 nm) and most active in the reaction of in CO oxidation [5].*

The physical and chemical (catalytic) properties of small metal particles in all known investigations were determined for arrays characterized by a quite wide size distribution of particles Thus, it is still unclear whether information on averaged properties and characteristics of samples corresponds to their possibly small part (e.g., most disperse) that is responsible for anomalous physical and chemical properties. In view of the above discussion, it seems promising to use cucurbit[*n*]uril as “hosts” for monodisperse metallic “guests.” Organic capsules of cucurbituril (organic molecules $C_{6n}H_{6n}N_{4n}O_{2n}$ (CB[n]), n = 5 – 10) are the most suitable for “calibrating” by size and shape nanoparticles ≤ 1 nm.

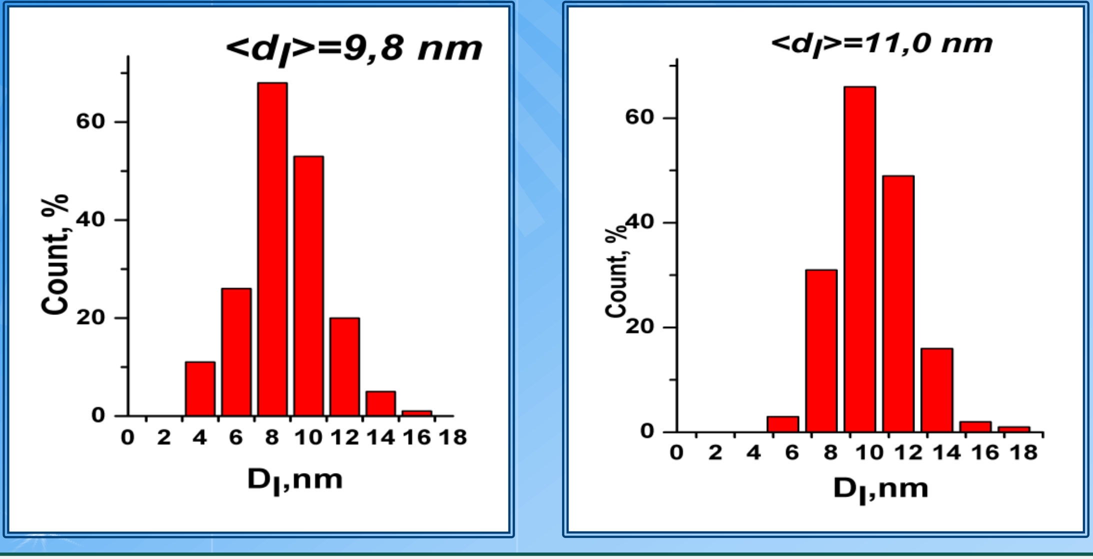

Fig.3. *Bar chart of Au- nanoparticles size distribution calculated from TEM for samples Au on* Al_2O_3*:* ***a*** *(left) and* ***b*** *(right). This samples are characterized by simile mean sizes, but differ in the presence of dispersive Au that are responsible for activity in CO oxidation .*

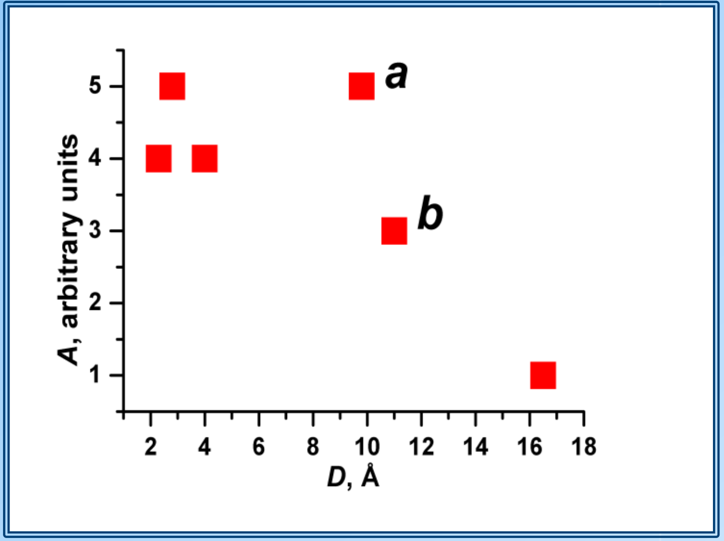

Fig.4. *Catalytic activity in CO oxidation based on surface gold atoms (A, arbitrary units) as a function of the mean gold particle diameters (D, Å) determined by TEM.*

Schema of cucurbit[n]urils molecules, $(C_6H_6N_4O_2)_n$, CB[*n*]

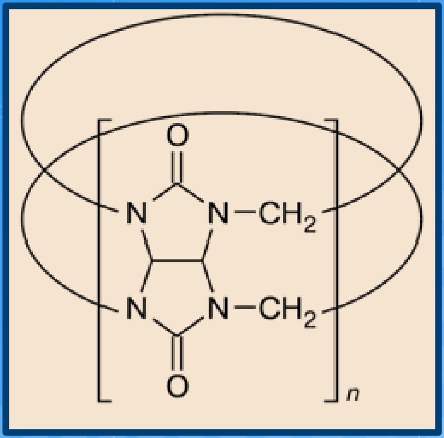

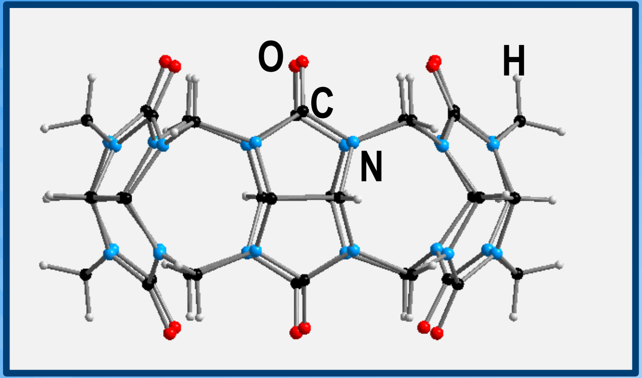

CB[6], $C_{36}H_{36}N_{24}O_{12}$

Lee J.W., Samal S., Selvapalam N. et al. Acc. Chem. Res. 2003, 36 (8), 621.

W.A. Freeman at al, J. Am. Chem. Soc. 1981, 103, 7367.

CB[*n*]: n=5 – 10, n – number of chain links

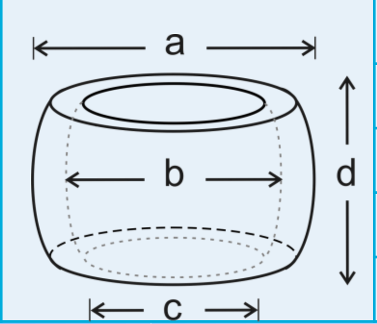		CB[5]	CB[6]	CB[7]	CB[8]	CB[10]
	Cavity diameter - b, Ǻ	4.4	5.8	7.3	8.8	10.7 – 12.6
	Entrance diameter - c, Ǻ	2.4	3.9	5.4	6.9	9.0 – 11.0
	Height - d, Ǻ	9.1	9.1	9.1	9.1	9.1
	Cavity volume - v, Ǻ³	82	164	280	480	870

Preparation of Au@CB[7]

Gold nanoparticles were encapsulated by using liquid-phase process that involved solutions of CB[7]s in water/ethanol mixture with various $HAuCl_4$+CB[7] concentration in solution (10^{-3} and 10^{-4} mol/L) and the reduction of $HAuCl_4$ by $NaBH_4$. For dissolution CB[6] in water and obtaining the Au@CB[6]- inclusion compound was used $MgCl_2$. After reduction the solution became immediately colored, which indicated the of Au^{III} to form gold nanoparticles. (In accordance with publication A. Corma, H. Garc´ia, P. Montes-Navajas et al., Eur. J. B **13**, 6359 (2007)).

Samples		**Initial compounds**			
		$HAuCl_4$, CB[7], mol/L	**Water:ethanol**	**$NaBH_4$, mol/L**	**$MgCl_2$**
1	CB[7]	**10^{-3}**	1:1	0.1	
2	CB[7]	10^{-4}	1:1	0.1	
3	CB[7]	10^{-4}	**1:0**	0.1	
4	CB[7]	10^{-4}	1:1	0.1	
5	CB[6]	10^{-4}	**1:0**	0.1	+

The mean size of the Au particles in cucurbit[7]uril (Au@CB[7]) was determined from TEM micrographs

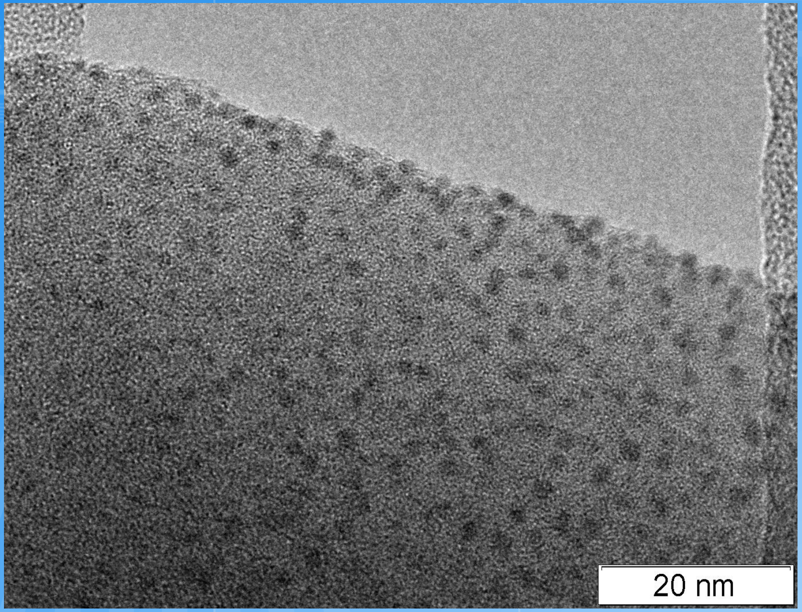

Fig.5. *TEM photo for sample 2.*

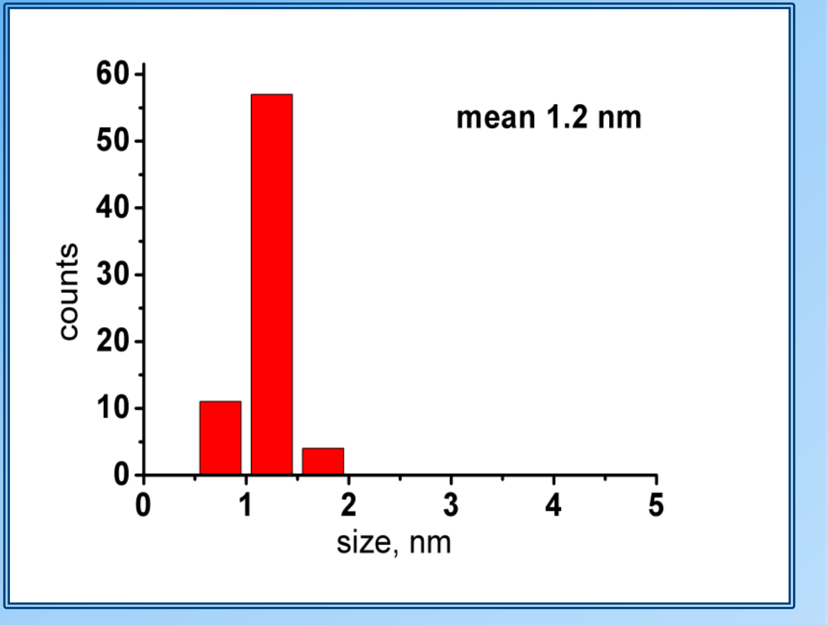

Fig.6. *Bar chart of Au- nanoparticles size distribution calculated from TEM photo for sample 2.*

Figures show the transmission electron microscope (TEM) image and size distribution histogram of gold nanoparticles for ultradisperse sample 2 obtained at an $HAuCl_4$ concentration of about 10^{-4} mol/L. For coarser disperse sample 1 obtained at an $HAuCl_4$ concentration of about 10^{-3} mol/L, the average size of Au clusters according to the TEM measurements is d ~ 10 nm, which is much larger than the size of cucurbit[7]uril cavities.

The mean size of the Au particles in cucurbit[7]uril (Au@CB[7]) was determined from TEM micrographs

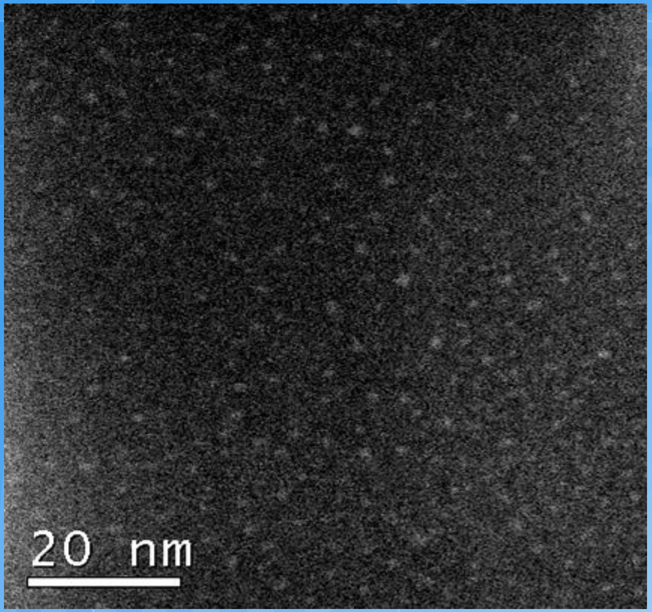

Fig.7. *TEM photo for sample 4.*

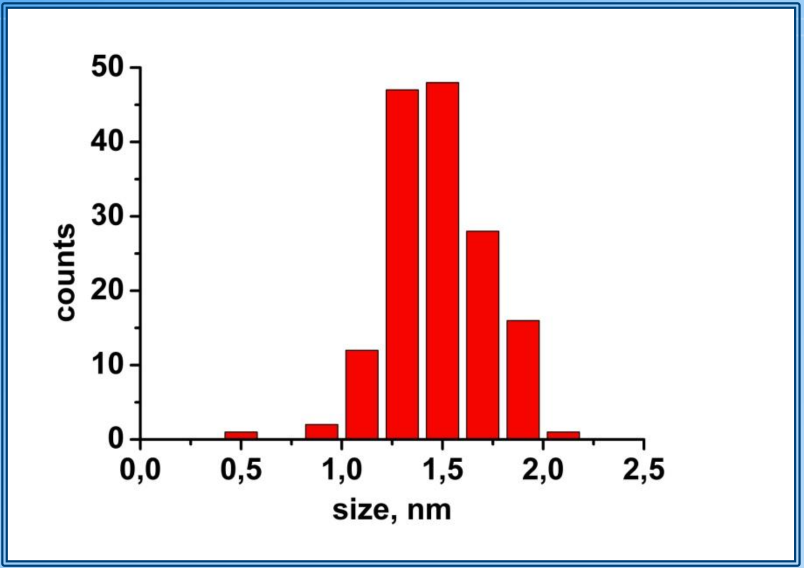

Fig.8. *Bar chart of Au- nanoparticles size distributions calculated from TEM photo for sample 4 (CB[7]).*

Figures show the transmission electron microscope (TEM) image and size distribution histogram of gold nanoparticles for disperse sample 4 (Au@CB[7]) obtained at an $HAuCl_4$ concentration of about 10^{-4} mol/L. For coarser disperse sample 3 obtained in several other conditions (water solution without ethanol) the average size of Au clusters according to the TEM measurements is $d \sim 6$ nm, which is much larger than the size of cucurbit[7]uril cavities.

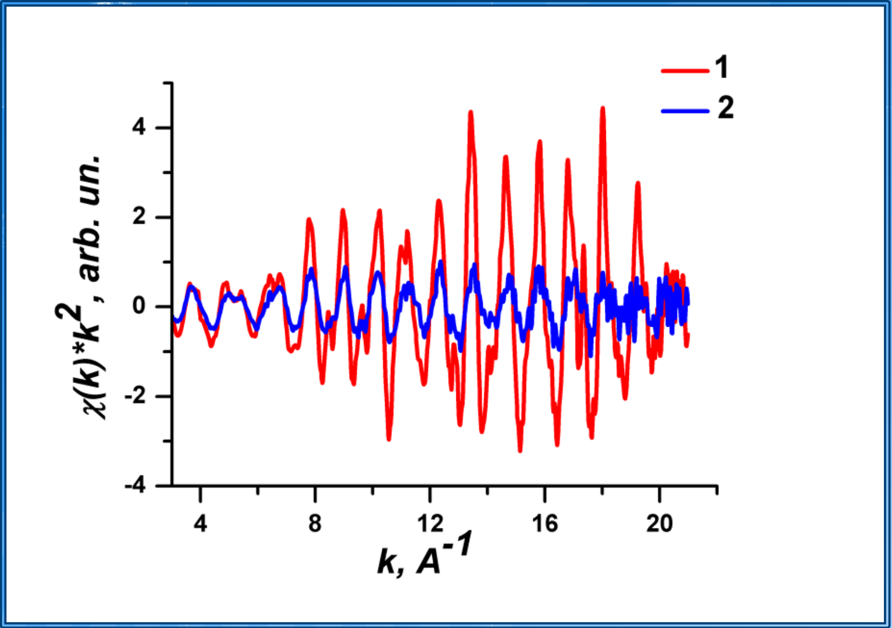

Fig.9. *Experimental $k^2\chi(k)$ AuL_{III} EXAFS spectra (k^2-weighted) of the 1, 2 samples measured at 12 K.*

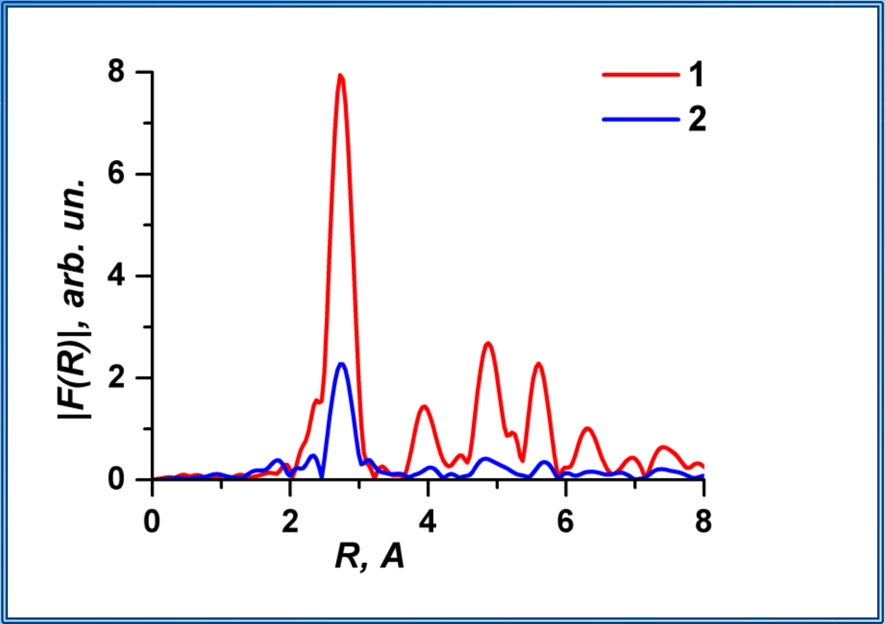

Fig.10. *Fourier transform magnitude |F(R)| of $k^2\chi(k)$ AuL_{III} EXAFS spectra of the 1, 2 samples measured at 12 K.*

It can be seen that the measurement at low temperature (12 K) were recorded with high statistics and in a fairly wide range of wave vectors (ID 26). Oscillations of the fine structure of the absorption spectra and maximums *Fourier transform magnitude* |*F(R)*| are much more pronounced for sample 1; this property is characteristic of spectra of coarser disperse particles and bulk foil.

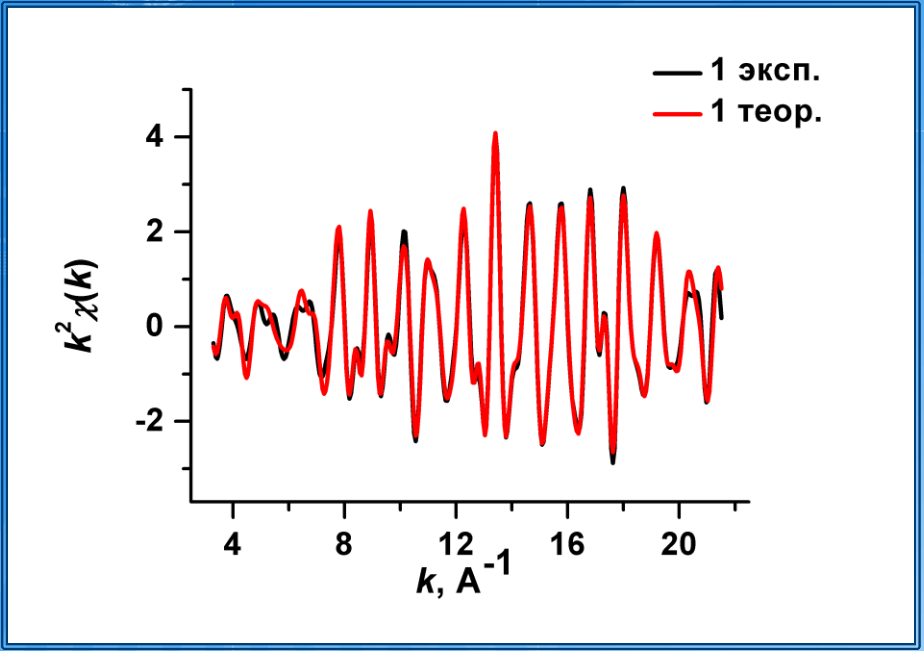

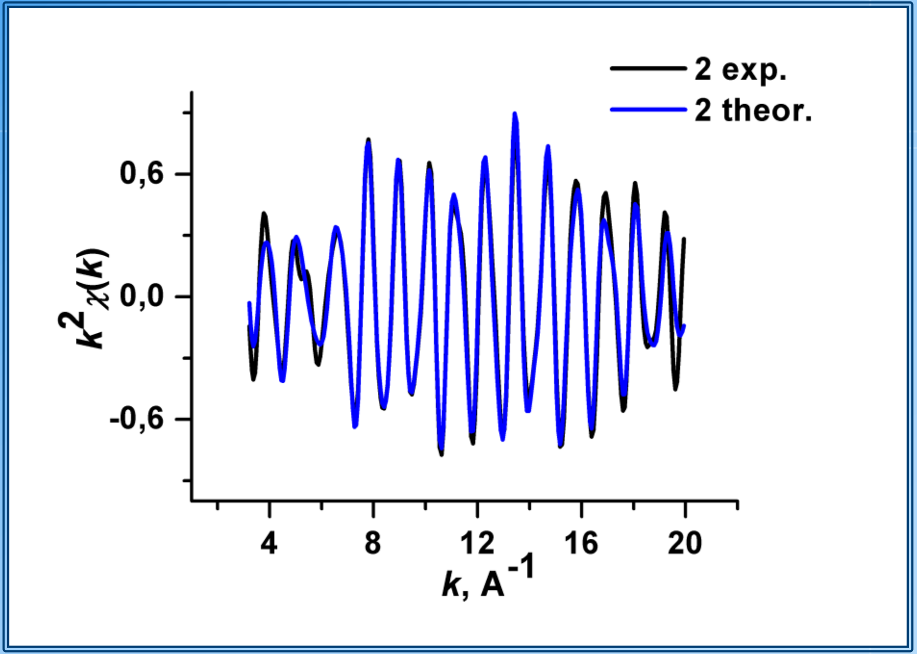

Fig.11. *The* Fourier-filtered (ΔR=2 - 6.5 Å, 5 shells) *$k^2\chi(k)$ AuL_3 EXAFS function (T=12 K) of the 1 sample: black line – experiment; red line – EXCURV 98 - fitting.*

Fig.12. *The Fourier-filtered (ΔR=2 - 5.4 Å, 3 shells) $k^2\chi(k)$ AuL_3 EXAFS function (T=12 K) of the 2:sample: black line – experiment; blue line – EXCURV 98 - fitting.*

Figures 12, 13 show sufficiently good agreement between the experimental and model spectra $k^2\chi(k)$ AuL_3 for both samples.

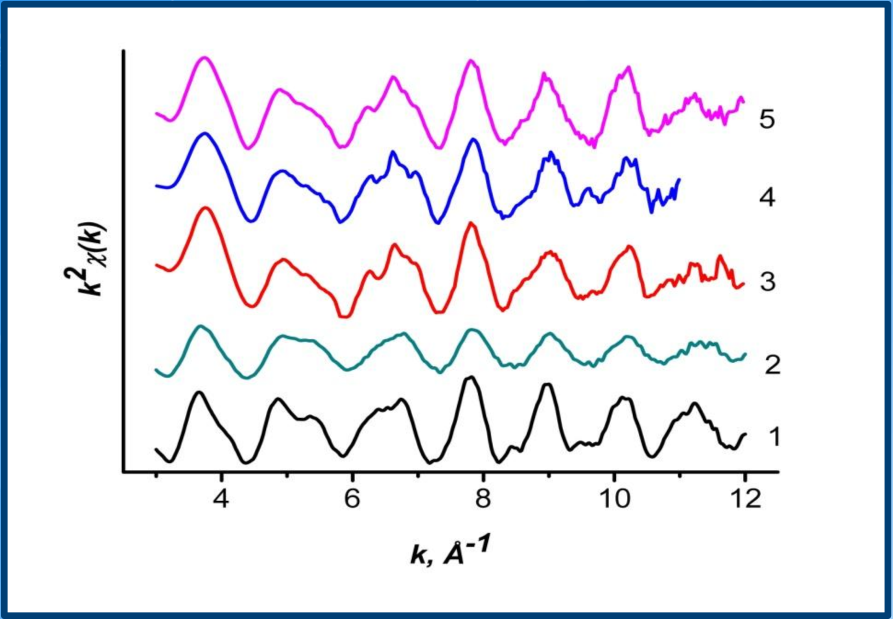

Fig.13. *Experimental* $k^2\chi(k)$ *Au*L_{III} *EXAFS spectra of the 1 -5 samples measured at room temperature .*

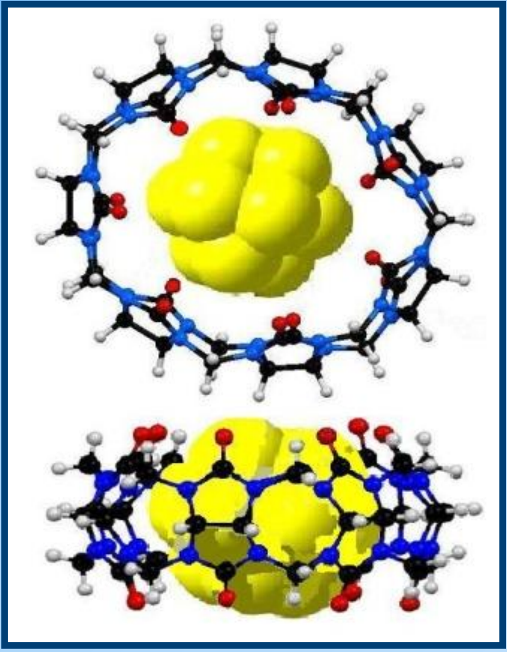

Au@CB[7]

Table 1. AuL_{III} $k^2\chi(k)$ EXAFS data fit parameters for the samples 1-5 and Au foil.

N_1 - the mean coordination numbers Au-Au, R_1 - the interatomic distances Au-Au, σ^2 - the Debye-Waller factor, F_{EXAFS} – goodness of fit.

ΔR=1.5 – 3.2 Å; S_0^2=0.82

Sample		Δk, Å^{-1}	N_1	R_1, Å	$2\sigma^2$, Å^2 297 K	$2\sigma^2$, Å^2 12 K	F_{EXAFS}
1	CB[7]	3-20	11.9	2.87	0.017	0.0045	0.4
2	CB[7]	3-20	6.7	2.84	0.023	0.0073	1.4
3	CB[7]	3-12	11.2	2.87	0.020		3.1
4	CB[7]	3–12	9.2	2.85	0.018		2.7
5	CB[6]	3-12	10.0	2.86	0.020		5.2
Au_foil		3-22	12	2.872	0.016	0.0026	0.4

Comparison of fitting results for models with one (left) and two (right) maximums of size distribution (bi-dispersive model)

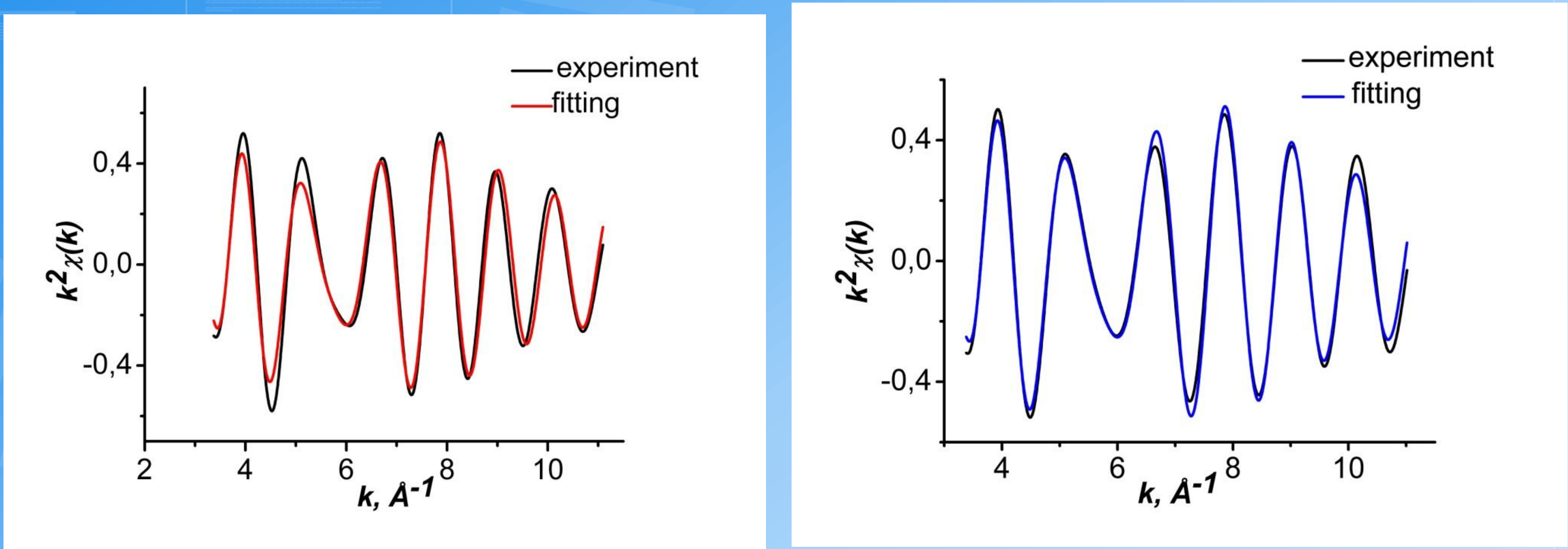

$F_{\mathrm{EXAFS}}=2.7$

$F_{\mathrm{EXAFS}}=1.4$

Fig.14. *The* Fourier-filtered (ΔR=1.5 - 3.5 Å) *experimental (T=297 K) and model* $k^2\chi(k)$ *AuL*$_3$ *EXAFS functions for the sample 4*.

Table 2. AuL_{III} $k^2\chi(k)$ EXAFS data fit parameters the samples 2, 4, 5 for model with two maximums of size distribution (bi-dispersive model)

$N_{1,2}$ - the coordination numbers, $R_{1,2}$ - Au-Au interatomic distances, σ^2 - the Debye-Waller factor, F_{EXAFS} - the fit index (goodness of fitting) for bi-dispersive model. Red color figures correspond to the fixed values of N_1 and R_1. ΔR=1.5 – 3.2 Å; S_0^2=0.82

Sample		N_1	N_2	R_1, Å	R_2, Å	$2\sigma^2$, Å^2	F_{EXAFS}
2	CB[7]	**12** **(15%)**	**6.1** **(85%)**	**2.87**	2.84	0.022	2.2
4	CB[7]	**12** **(65%)**	**5.7** **(35%)**	**2.87**	2.84	0.018	1.4
5	CB[6]	**12** **(89%)**	**5.1** **(11%)**	**2.87**	2.84	0.020	4.5

The size dependent average coordination number (CN) of a 12-fold coordinated spherical Au nanoparticle (NP) can be estimated by

$$\boxed{CN_{NP} = 12\left(1 - \frac{3}{2D} R_{nn}\right)} \Rightarrow \boxed{D = \frac{3}{2} \times \frac{R_{nn}}{1 - CN_{NP}/12}}$$

R_{nn} is the bond length, D – the average NP diameter and CN_{NP} – NP coordination number [P. Kluth, B. Johannessen, G.J. Foran, D.J. Cookson, S.M. Kluth, M.C. Ridgway. *Disorder and cluster formation during ion irradiation of Au nanoparticles in* SiO_2. Phys. Rev. B, **74**(1), 2006. P. 014202(9)].

R_{nn}=2.84 Å: CN_{NP} ~ 6 – D ~ 8 Å, CN_{NP} ~ 5 – D ~ 7 Å

This estimate is several understated for particles containing a small number of atoms due to the spherical approximation

High Energy Resolution Fluorescence Detected X-ray Absorption Spectroscopy (HERFD XAS): Selection of a specific fluorescence line to perform XANES measurements, using a high resolution X-ray spectrometer, with an energy resolution specified by the core - hole lifetime for the detected emission. HERFD spectra were measured at the ID26 beam-line of the ESRF, Grenoble.

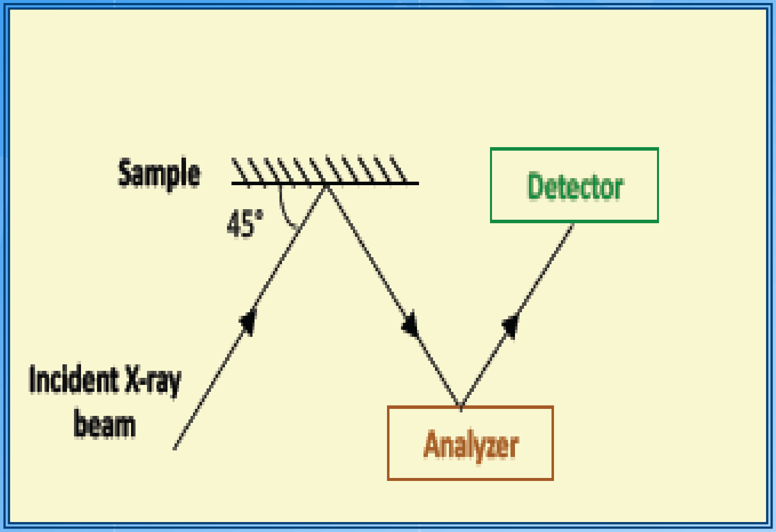

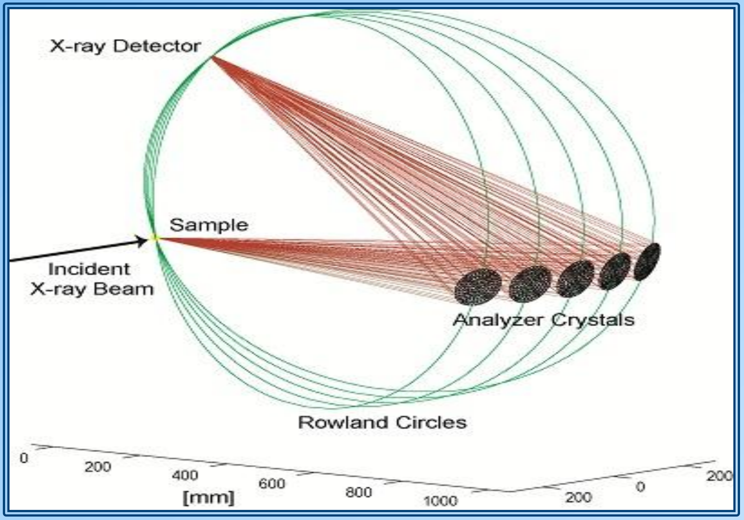

HERFD XAS experiment scheme

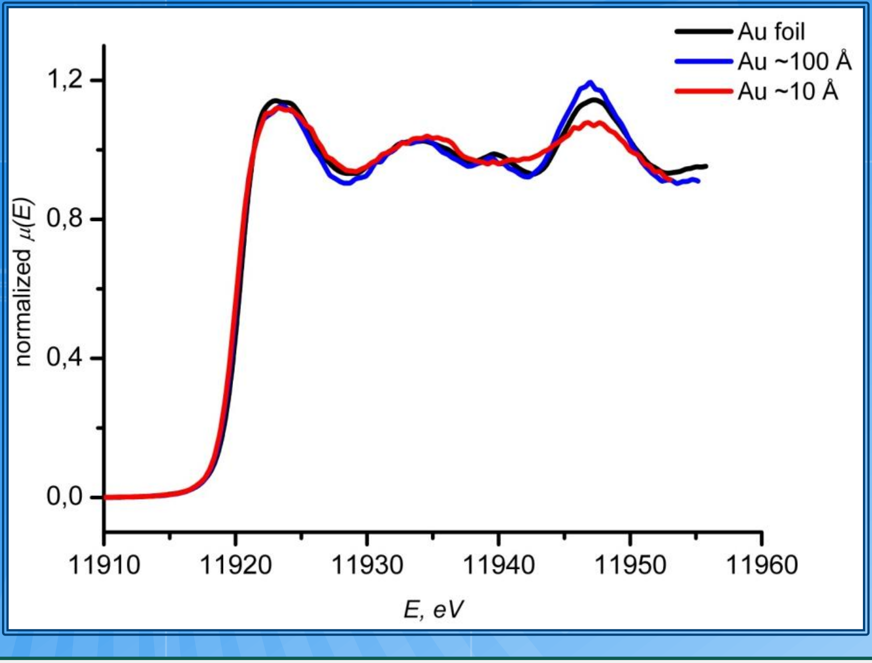

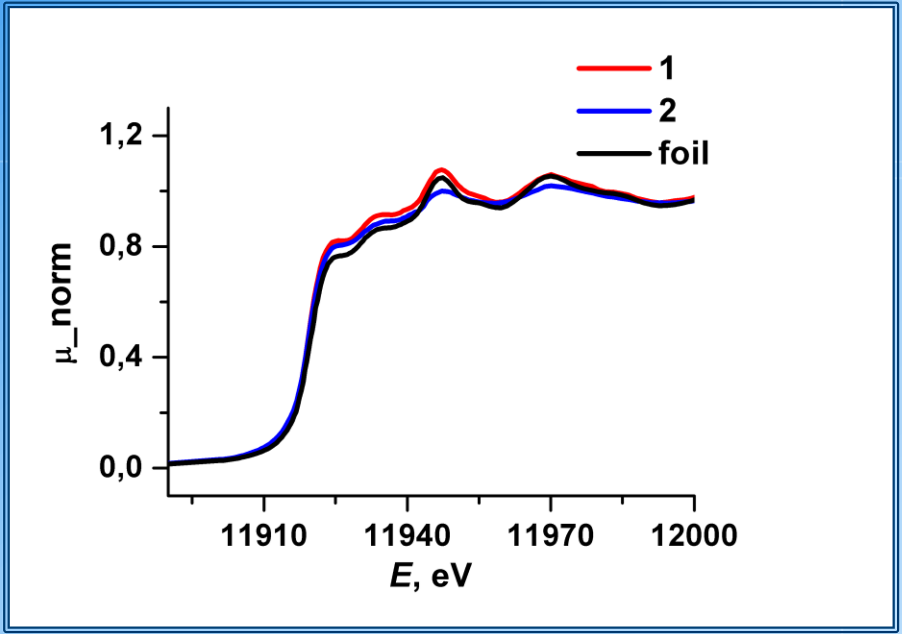

Fig.15. *Experimental AuL_3 HERFD XAS spectra (T = 12 K) for samples 2 (red line), 1 (blue) and gold foil (black).*

Fig.16. *Experimental AuL_3 XANES spectra (T = 12 K) for samples 2 (red line), 1 (blue) and gold foil (black).*

The analysis of the shapes of the HERDF XAS and XANES spectra shows that the intensities of the main (first) maximum A beyond the Au L_3 absorption edge for these samples coincide within the accuracy of our experiments and data processing (~5%). Thus, in agreement with the accepted interpretation of such maxima, the charge state and number of free electron states above the Fermi level remain unchanged for these samples within the accuracy of our measurements; i.e., the electron state of such gold particles is the same as for bulk metal samples within our accuracy.

Models for FEFF- calculation of small clusters with sizes correspond to cucurbituril CB(6,7) cavities

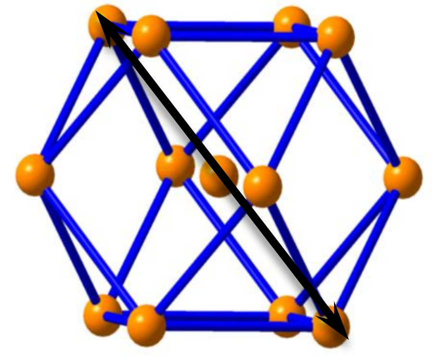

globule
b=8.64Å,
N_{cn}=5.54

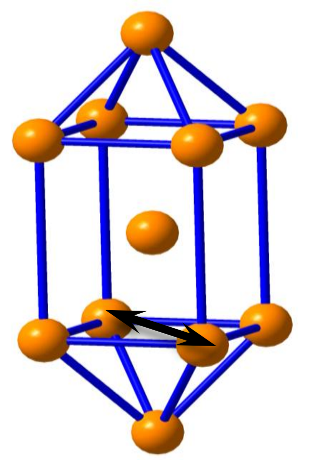

pyramid
b=6.95Å
N_{cn}=4.73

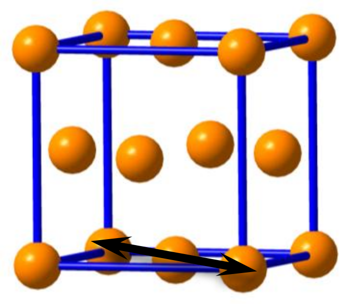

cubic
b=8.64Å
N_{cn}=5.1

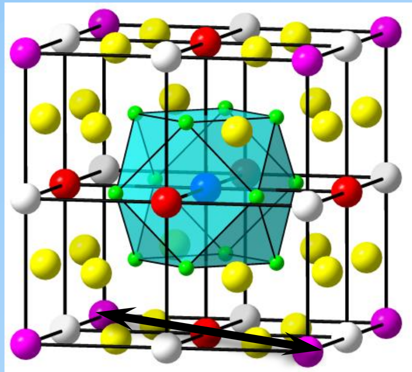

cubic
b=14.4Å
N_{cn}=7.62

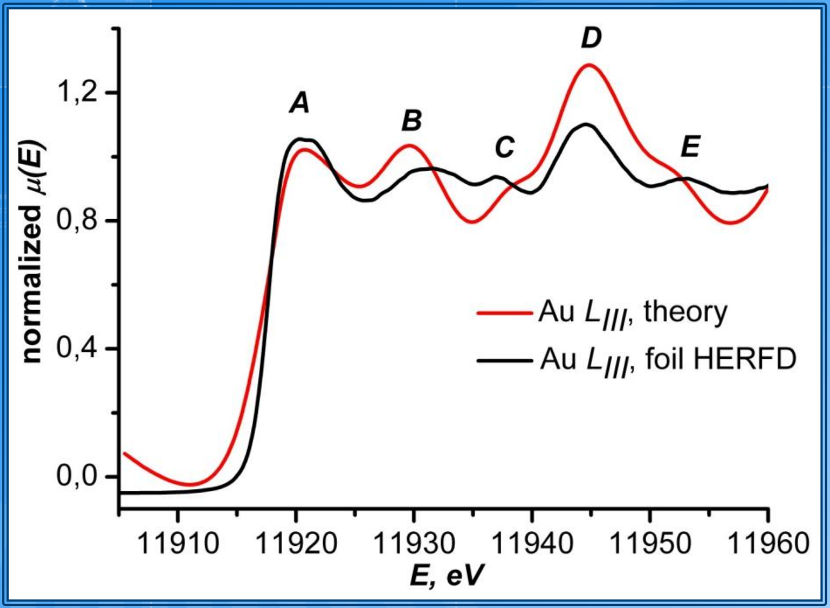

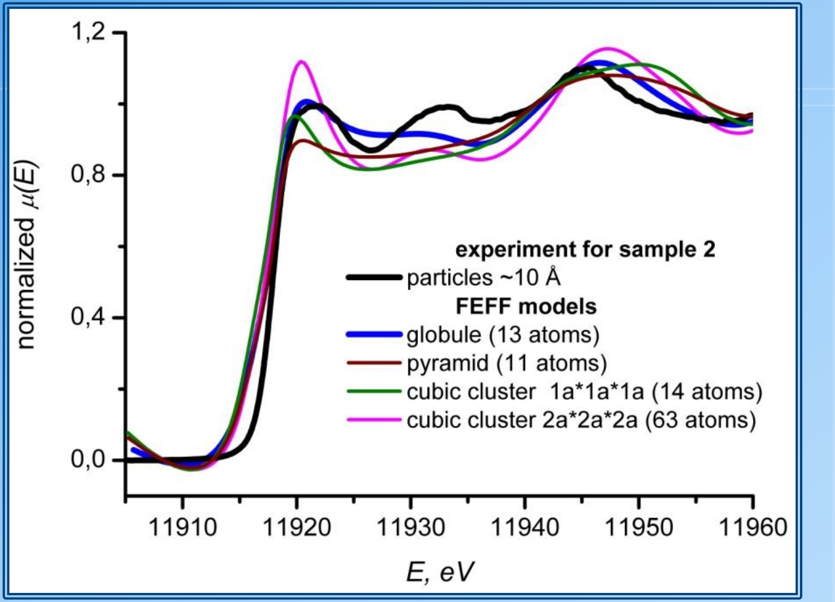

Fig.17. *Comparison of AuL_{III} XANES curves: FEFF-calculated and HERFD-experimental for Au foil (bulk Au)*

Fig.18. *Comparison of AuL_{III} XANES curves: FEFF-calculated for models (globule, cubic, pyramid clusters) and HERFD-experimental for sample 2*

In accordance with Fig.18 the better agreement with experiment gives symmetric «globule»- model. Special properties of atoms on the surface of small gold particles apparently are not determined by their position at the vertices and edges of small clusters

Summary and Conclusions

- It has been found, that gold clusters in cavities of cucurbit[7]uril are characterized by smaller (0.03Å) interatomic distances and as compared to bulk gold and a considerable reduction in the first shell Au-Au coordination numbers ($N_{Au\text{-}Au} \leq 6$).
- It has been found for all samples that Au clusters size distribution have two maximums:

1) finely divided Au within the cavities of cucurbituril molecules with narrow size distribution and 2) larger particles of gold.

- Fitting the EXAFS spectra measured at 12 K permits detecting large (threefold) increase of the Debye-Waller factor for the most dispersed samples Au@CB[7] in comparison with bulk metal and correspondingly the valuable increase in the structural disorder for the smallest Au particles in comparison with the bulk Au metal.
- No visible differences in electron states of Au for samples Au@CB[6,7] and the bulk Au metal were detected.
- Special properties of atoms on the surface of small gold particles apparently are not determined by their position at the vertices and edges of small clusters; they are likely attributed to the structural disorder, deformations, and stresses, which increase with a decrease in the size of the particles.
- These new results are in accordance with our results obtained previously for the samples prepared by other methods and containing Au particles with bigger sizes and more wide size distributions [2,4].

Institute of Inorganic Chemistry SB RAS

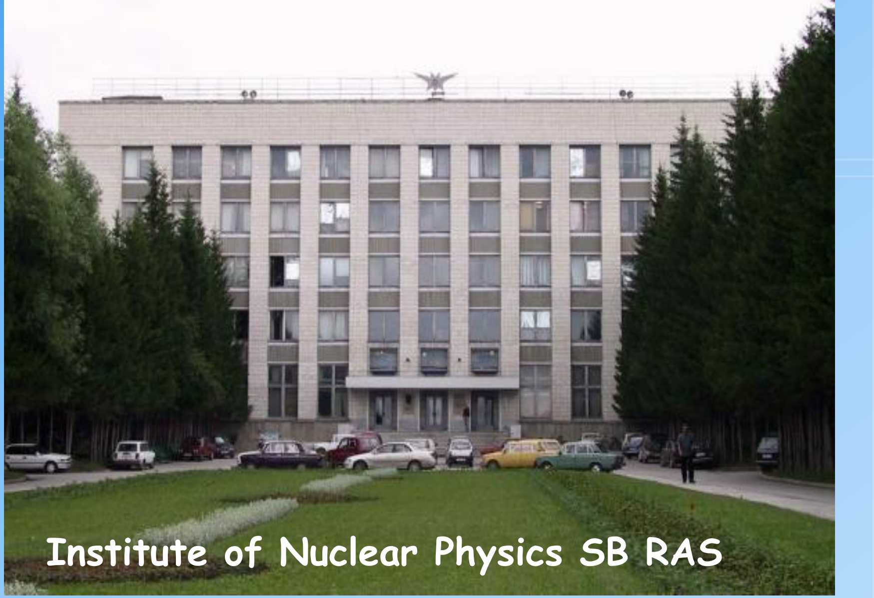

Institute of Nuclear Physics SB RAS

Thank you for attention!

Institute of Catalysis SB RAS

ESRF, Grenoble, France